MOLECULAR AND CELLULAR BIOLOGY, Feb. 2006, p. 1087–1097 Vol. 26, No. 3
0270-7306/06/$08.00+0 doi:10.1128/MCB.26.3.1087–1097.2006

Oxidative Stress-Responsive Transcription Factor ATF3 Potentially Mediates Diabetic Angiopathy

Aki Okamoto,[1,2] Yasuhiko Iwamoto,[2] and Yoshiro Maru[1]*

Department of Pharmacology[1] and Diabetes Center,[2] Tokyo Women's Medical University, 8-1 Kawada-cho, Shinjuku-ku, Tokyo 162-8666, Japan

Received 31 May 2005/Returned for modification 12 July 2005/Accepted 8 November 2005

Previous results of our cDNA microarray analysis to look for genes whose expression level correlates well with in vitro tubulogenesis by NP31 endothelial cells revealed the transcription factor ATF3 known to be responsive to stress such as reactive oxygen species (ROS). Anti-ATF3 small interfering RNA gave an inhibitory influence on tube formation by NP31 cells expressing an activated form of the vascular endothelial growth factor receptor 1 (VEGFR-1) kinase. When expression of ATF3 was regulated under the control of tetracycline system in NP31 cells, they acquired the tubulogenic ability upon ATF3 induction. While ATF3 failed to induce expressions of VEGF and VEGFR, it regulated those of CDK2, CDK4, p8, plasminogen activator inhibitor 1, integrin α1, subunit and matrix metalloprotease MMP13. In H_2O_2-stimulated NP31 cells as well as endothelial cells of glomerulus and aorta of Otsuka-Long-Evans-Tokushima-Fatty diabetic model rats, concomitantly enhanced expressions of ATF3, PAI-1, and p8 were observed. Given the proposed hypothesis of the close linkage between diabetic angiopathy and ROS, those data suggest that ROS-associated diabetic complication may involve ATF3-mediated pathological angiogenesis.

Diabetic complications are characterized by microvascular diseases especially in the retina, glomerulus, and vasa nervorum. It involves apoptosis and remodeling of endothelial cells. Canonically, hyperglycemia is an essential cause of reactive oxygen species (ROS)-mediated oxidative stress in this complication (4). Evidence to show the linkage between oxidative stress and behaviors of endothelial cells is accumulating, which includes migration and tube formation by hydrogen peroxide (H_2O_2) in vitro (35, 40), in vivo angiogenesis in experimental atheroma possibly caused by ROS-induced production of vascular endothelial growth factor (VEGF) (17, 25), and so forth. Our recent report that plasminogen activator inhibitor 1 (PAI-1) is ROS-dependently expressed in white adipocytes in hyperglycemic Otsuka-Long-Evans-Tokushima-Fatty (OLETF) diabetic model rats lends more credence to this increasingly accepted hypothesis (42). PAI-1-deficient mice revealed abnormalities in aortic endothelial cells (34). However, the signaling pathways of oxidative stress in endothelial cells are poorly understood.

We have previously reported an establishment of a nontubulogenic endothelial cell line NP31 derived from sinusoidal endothelial cells of rat liver (21). NP31 cells formed tubules with a lumen in Matrigel when a constitutively activated form of VEGF receptor 1 (VEGFR-1) (Flt-1) kinase, BCR-FLTm1, was expressed (NP31/kinase cells) (22, 23). By applying cDNA microarray analysis to those nontubulogenic and tubulogenic cells in a variety of culture conditions to look for gene(s) whose mRNA expression levels are up-regulated in tubulogenic conditions, we found the oxidative stress-responsive transcription factor ATF3 with high scores (18).

ATF3 is a member of the ATF/CREB transcription factor family with at least 5 naturally occurring isoforms derived from alternative splicing (5, 12, 31, 46). For example, ATF3ΔZip that is devoid of the leucine zipper domain does not appear to bind to DNA but still retains corepressor-binding activity (5, 31). The ATF3 isoforms can heterodimerize with each other and with other transcription factors such as c-Jun, ATF2, Smad3, and so forth. Depending on its partner, target promoter, or cellular context, ATF3 functions either as a transcriptional activator or repressor. One of the ATF3 targets of repression is Id1, which regulates angiogenesis by changing expression levels of thrombospondin 1 and VEGF (3, 14, 45). Growth suppression has been reported in HeLa cells by overexpression of ATF3 (9). ATF3 expression has also been found in the atherosclerotic lesion where endothelial cells are under programmed cell death (27).

In this report we directly examine the ATF3 activities in endothelial tubulogenesis and cell growth and its potential transcription targets in in vitro and in vivo models of diabetic animals.

MATERIALS AND METHODS

Cell cultures. COS7 cells were cultured in Dulbecco's modified Eagle's medium supplemented with 10% fetal calf serum. NP31/kinase cells and their conditions in usual liquid or Matrigel cultures were described before (23). The tetracycline (Tet) regulatory system was established in NP31 cells with the pUHD10-3 internal ribosome entry site green fluorescent protein vector (8) kindly provided by Owen Witte (University of California—Los Angeles). Three independent clones in which ATF3 expression was clearly regulated by Tet were eventually isolated (NP31/ATF3-Tet cells), and they behaved in a similar fashion. To establish NP31/ATF3-Tet cells expressing an activated form of the VEGFR-1 kinase from a single cell, one representative NP31/ATF3-Tet cell clone was infected with BCR-FLTm1 retrovirus (22) and plated into soft agar before several macroscopic colonies were picked up and plated back into liquid culture. All of them not only expressed BCR-FLTm1 but also were capable of inducing ATF3 in a Tet-regulated manner (NP31/kinase/ATF3-Tet cells). For induction of the endogenous ATF3 in NP31 cells, cells were stimulated with tumor necrosis factor alpha (TNF-α) at 10 ng/ml, transforming growth factor β (TGF-β) at 20 ng/ml, or H_2O_2 at 100 μM.

* Corresponding author. Mailing address: Department of Pharmacology, Tokyo Women's Medical University, 8-1 Kawada-cho, Shinjuku-ku, Tokyo 162-8666, Japan. Phone and fax: 81-3-5269-7417. E-mail: ymaru@research.twmu.ac.jp.

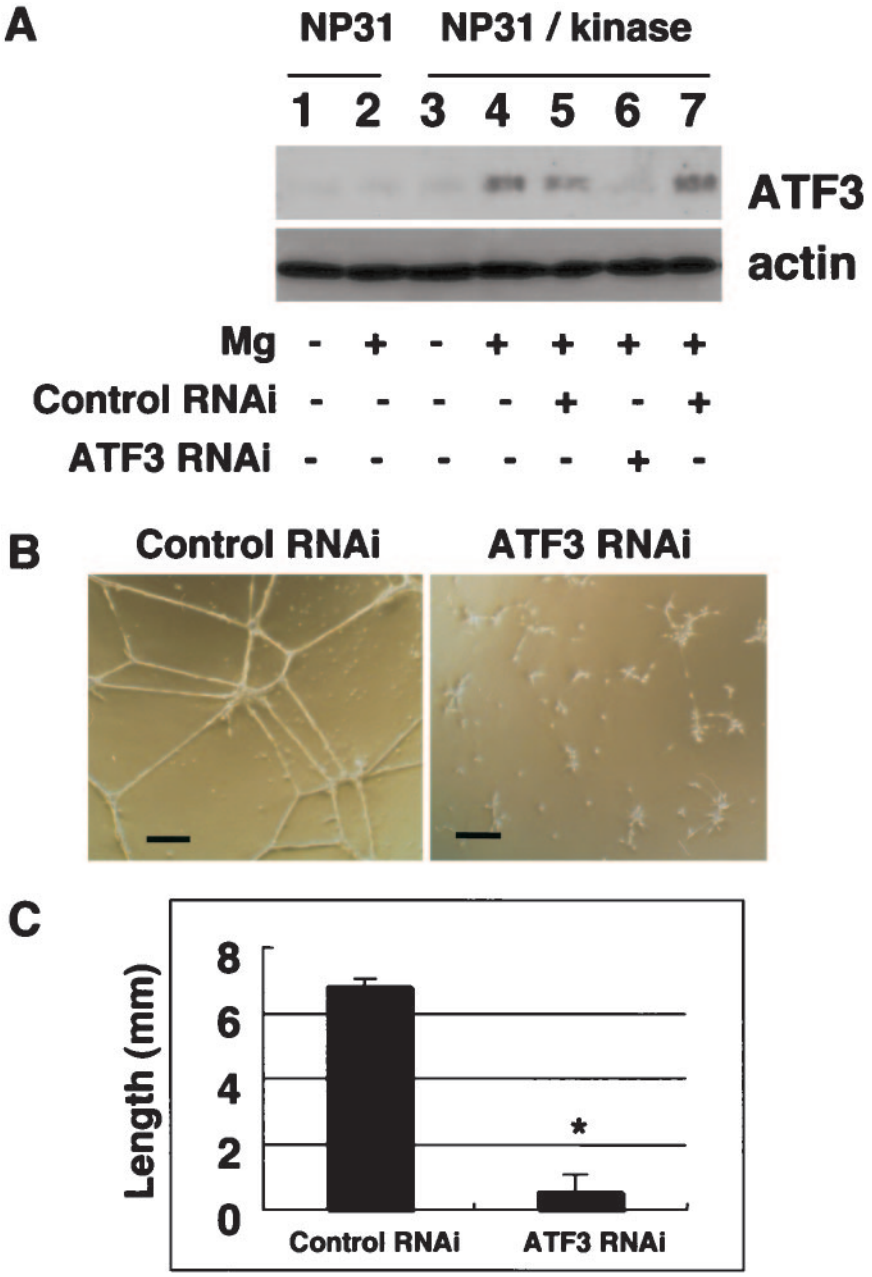

FIG. 1. (A) NP31 or NP31/kinase cells were untreated (lanes 1 to 4) or pretreated with either anti-ATF3 siRNA (lane 6; antisense/sense) or its control (lane 5; sense/sense) and anti-Nox1 siRNA (lane 7; antisense/sense) before plating onto Matrigel-coated dishes (Mg) (lanes 2, 4 to 7). Total protein lysates were subjected to anti-ATF3 (upper panel) and antiactin (lower panel) Western blotting. (B) Cells corresponding to lanes 5 and 6 in panel A were subjected to in vitro Matrigel assays. Bars, 100 μm. (C) Quantification of in vitro tubule formation in panel B. Means ± SD of results from three independent experiments are shown. +, present; −, absent; *, $P < 0.05$ versus control RNA interference (RNAi).

In vitro angiogenesis assay in Matrigel. Quantification of the length of cords in branching morphogenesis was performed as described previously (19). In NP31/ATF3-Tet cells, cells were plated onto Matrigel after removing Tet for the indicated period of time. Statistical results were expressed as means ± standard deviations (SD) of the results from three or four independent experiments. Statistical significance was evaluated by one-way analysis of variance, followed by Bonferroni/Dunn's test. A P value of <0.05 was accepted as significant.

RNA extraction and reverse transcriptase-mediated PCR (RT-PCR) analysis. Total cellular RNA was extracted by Isogen (Invitrogen), followed by the cDNA synthesis by SuperScript (Invitrogen). Approximately 5- by 5- by 5-mm pieces of each organ in Isogen solution were homogenized in a glass homogenizer before the addition of chloroform. For preparation of glomeruli, the kidney cortex cut into small pieces was subjected to 3 rounds of filtration through stainless steel mesh screens with 3 different pore sizes as described by Karnovsky and Ryan (15). Primers were ′-CAACATCCAGGCCAGGTCTGT-3′ (forward) and 5′-GCGGCCGCCTCTGCAATGTTCCTTCTTTT-3′ (reverse) for rat ATF3, 5′-AACAGGCAAGACTTTGGAG-3′ (forward) and 5′-GTTGTACAGTTTATTGTTACTG-3′ (reverse) for rat p8, 5′-ATGAACTTTCTGCTCTCTTGGGT-3′ (forward) and 5′-GAACATTTACACGTCTGCGGATC-3′ (reverse) for rat VEGF-A, 5′-CCAAGATGCTATGCCATTCA (forward) and 5′-ACTTGTTGTTCTGAGCCATC-3′ (reverse) for rat PAI-1, 5′-CAAGAAATGCAGCAAGACCA-3′ (forward) and 5′-CCGGGCTGGAGTACTATGAA-3′ (reverse) for rat CYR61, and 5′-GCCAAGGTCATCCATGACAA-3′ (forward) and 5′-GTTTCTTACTCCTTGGAGGC-3′ (reverse) for rodent glyceraldehyde-3-phosphate dehydrogenase (GAPDH).

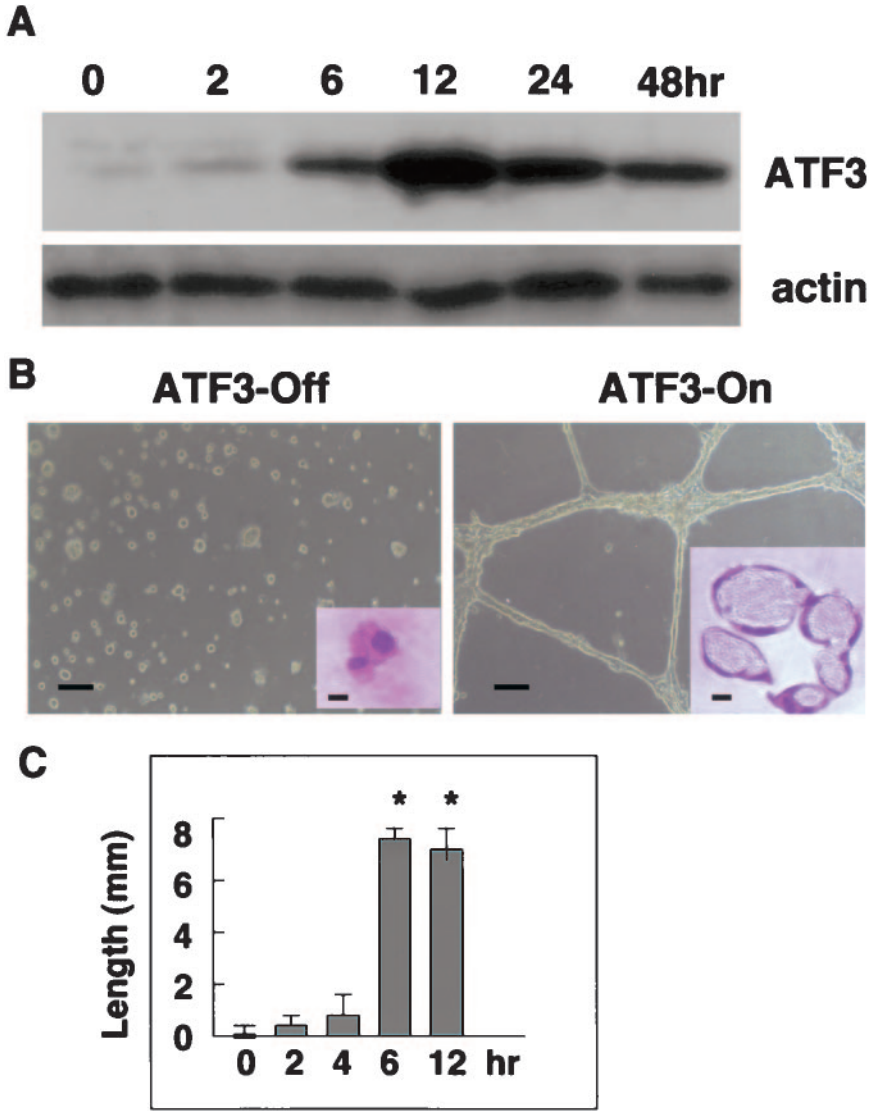

FIG. 2. (A) NP31/ATF3-Tet cells were deprived of Tet for the indicated time. Total protein lysates of each time point were subjected to anti-ATF3 (upper panel) and antiactin (lower panel) Western blotting. (B) NP31/ATF3-Tet cells were left untreated (ATF3-Off, left panel) or deprived of Tet for 12 h (ATF3-On, right panel) before plating onto Matrigel. Microscopic pictures were taken 12 h after plating. Bars, 20 μm. The insets show their histological sections stained by hematoxylin-eosin. Bars, 10 μm. (C) NP31/ATF3-Tet cells were deprived of Tet for the indicated number of hours before quantification of in vitro tubulogenesis was performed. Means ± SD of results from three independent experiments are shown. *, $P < 0.05$ versus time zero.

To ensure normalization of the cDNA amounts, we also used another GAPDH primer pair (forward, 5′-CATTGTCTACTATGACGGAC-3′; reverse, 5′-GCAATTGTCATCTTCTCCCA-3′) and a β-actin primer pair (forward, 5′-ATGGATGATGATATCGCCGCG-3′; reverse, 5′-GGGCACAGTGTGGGTG ACCCC-3′), which we have previously utilized for NP31 cells (21). All sets of primers were initially tested with cDNA samples that were synthesized with or without reverse transcriptase, and resulting RT-PCR products were examined by DNA sequencing. For semiquantitative PCR, the linear range of measurement was established by trying different numbers of cycles (usually 15, 20, 25, 30, and 35). Results before saturation were shown for each gene.

siRNA-mediated knockdown experiments. Based on the rat ATF3 sequence, sense primer (S) (5′-GCACCUUUGCCAUGGGAUGTT-3′) and antisense primer (A) (5′-CAUCCGAUGGCAAAGGUGCTT-3′) were designed. A small interfering RNA (siRNA) for Nox1 has been described previously (19). Annealed primers were added to NP31/kinase cells by utilizing transfection reagent (TransIT-TKO; Mirus) and Opti-MEM (GIBCO). After incubation for 24 h, cells were plated onto Matrigel.

Plasmid construction, transfection, and reporter assay. V5-tagged constructs, V5-ATF3 (amino acids [aa] 1 to 181) and V5-ATF3ΔZip (aa 1 to 115) were generated by PCR and cloned in frame into the NotI and BamHI site of pcDNA4 containing V5 (Invitrogen). PCR primers, 5′-CCGCTCGAGGTCCCCAGTT AGGAGTCCCG-3′ and 5′-CCCAAGCTTGTGTTCTTCCCTCCAGCAA-3′, were used to amplify the human CDK2 promoter region originally described by Stennett et al. (39). The PCR product was subcloned into XhoI/HindIII sites of the pGL3 basic vector (Promega) to generate pCDK2-Luc. PCR primers, 5′-C GGGGTACCATGGGAAGTTGTGACTAATCCT-3′ and 5′-CCCAAGCTTG GGTGGCCATTATGCCTAGTCTGCT-3′, were used to amplify the −974 to +43 region of the mouse p8 promoter (GenBank accession no. AF131195) (43). The PCR product was subcloned into KpnI/HindIII sites of the same vector to generate pp8-Luc. All PCR products were verified by DNA sequencing. The PAI-1 promoter-luciferase fusion reporter construct pGL-3-PAI-1/full (−829 to +36) was kindly provided by S. Fujii at Hokkaido University (7).

Cos7 cells were seeded at 2×10^5 per well 20 h before transfection using Superfect reagent (QIAGEN). The reporter plasmid was cotransfected with

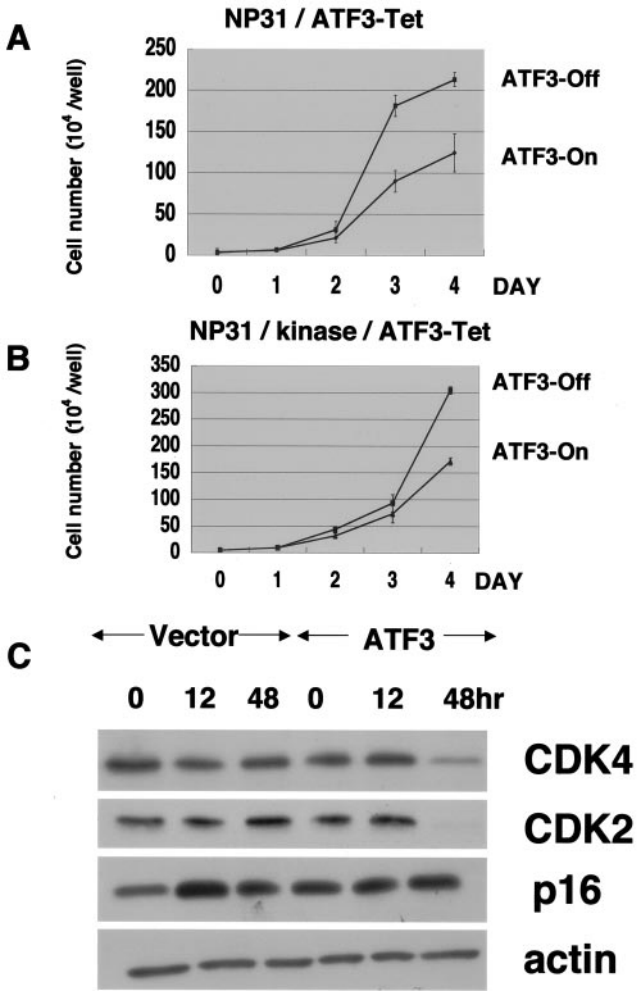

FIG. 3. Growth curves of NP31/ATF3-Tet cells (A) and NP31/kinase/ATF3-Tet cells (B) in the presence (ATF3-Off) or absence (ATF3-On) of Tet. Means ± SD of results from four independent experiments are shown. (C) NP31/ATF3-Tet cells (ATF3) or NP31 cells with just the Tet regulation vector (vector) were deprived of Tet for the indicated time before total protein lysates were subjected to anti-CDK4, anti-CDK2, anti-p16, and antiactin Western blotting. A representative blot from three independent experiments is shown.

either the V5-tagged full-length ATF3 or ΔZip in pcDNA4 (0.5 μg each). NP31/ATF3-Tet cells at 2×10^5 per well were also transfected with the reporter plasmid before and 24 h after ATF3 induction. In every case, 50 ng of pRL-SV40 (Promega) was added as an internal control. Cells were harvested 24 h after transfection, and luciferase activities were determined with the dual luciferase reporter assay system (Promega). Means of the results from six independent experiments were calculated. A statistical value of $P < 0.05$ is accepted as significant.

Antibodies and Western blotting. Polyclonal antibodies to ATF3, integrin α1, integrin β1, p53, Id1, p16, p21, p27, cyclinD1, CDK2, CDK4, MMP2, MMP9, and MMP10 were from Santa Cruz Biotechnology. Rabbit anti-rat PAI-1 antibody was from American Diagnostica. Monoclonal antibody against V5 was from Invitrogen, CD31 was from Pharmingen, and those against MMP13, RAGE, and actin were from Chemicon International. Anti-von Willebrand factor antibody was from Dako. Western blotting was performed as described previously (23). Briefly, cells were collected by cell scrapers, washed twice with phosphate-buffered saline (pH 7.4), and lysed with lysis buffers (50 mM HEPES, pH 7.4, 150 mM NaCl, 1% Triton X-100, 2 mM Na_3VO_3, 10 mM NaF, 10 mM pyrophosphate, 1 mM EDTA, 1 mM phenylmethylsulfonyl fluoride, 20 μg/ml leupeptin, 0.02% sodium dodecyl sulfate). Total lysates (approximately 20 μg each) were run on sodium dodecyl sulfate-polyacrylamide gel electrophoresis slab gels. The gel was transblotted on a nitrocellulose membrane (Amersham) and incubated with 5% bovine serum albumin for blocking. After incubation with appropriate antibodies, filters were subjected to washing and enhanced chemiluminescence Western blotting detection procedures (Amersham). The intensity of bands was quantified by NIH image. To compare the ATF3 protein levels, the ratios of the intensity of ATF3 bands relative to that of actin were calculated.

Animals. Male OLETF rats (body weight, 650 to 680 g), a model animal of type II diabetes mellitus, and male Long-Evans-Tokushima-Fatty (LETO) rats (450 to 500 g) for control ($n = 5$ each) were kindly provided by K. Kawano at Tokushima Research Institute, Otsuka Pharmaceutical Co., Japan (26). Mean values of plasma glucose concentration were 350 mg/dl and 127 mg/dl for OLETF and LETO rats, respectively, at the age of 25 weeks, when they were sacrificed. A dramatic elevation of PAI-1 expression was also observed only in OLETF rats at that age (42).

Histological analysis. Paraffin sections were dried for 24 h at 4°C, dewaxed with xylene twice (5 min), and passed through 96% ethanol twice (1 min) and Tris-buffered saline–Ca three times (5 min) before staining. These sections were preincubated in 0.1% bovine serum albumin for 1 h at 22°C and then incubated with an individual primary antibody at 4°C for 12 h, followed by incubation with a biotinylated secondary antibody (Vector) at 22°C for 1 h, a streptavidin-alkaline phosphatase (Dako) at 37°C for 15 min, and 5-bromo-4-chloro-3-indolylphosphate/nitroblue tetrazolium (Vector) at 22°C for 20 min. Triple staining of glomeruli was performed with mouse anti-rat CD31, rabbit anti-rat ATF3 (or rabbit anti-rat PAI-1), and Vectashield medium with propidium iodide (PI) for nuclei. Secondary antibodies were Cy5-conjugated goat anti-rabbit immunoglobulin G (for ATF3) and fluorescein isothiocyanate-conjugated goat anti-mouse immunoglobulin G (for CD31) (Jackson ImmunoResearch). Samples were analyzed under a Leica confocal laser-scanning microscope. Fluorescence images were presented by pseudocolors.

RESULTS

Inhibition of in vitro angiogenesis by anti-ATF3 siRNA. We have previously reported cDNA microarray analysis between nontubulogenic NP31 endothelial cells and tubulogenic NP31 cells expressing a constitutively activated form of the VEGFR-1 (Flt-1) kinase (BCR-FLTm1) (NP31/kinase cells) in Matrigel cultures. We found that expression of ATF3 mRNAs was induced by Matrigel in both of them, but the level of induction was much higher in NP31/kinase than NP31 cells as judged by semiquantitative RT-PCR analysis (18). This was supported by anti-ATF3 Western blotting shown in Fig. 1A (lanes 1 to 4). The induced expression of ATF3 at protein levels was prominent in NP31/kinase cells but not in NP31 cells. Among the ATF3 isoforms, the anti-ATF3 antibody used in our experiments can recognize only the full length (181 aa) and ΔZip2a,b (135 aa) but not others (5, 12, 31, 46). Considering the size of the detected band, we suppose that Matrigel induced at least the full-length ATF3 protein.

In usual cultures on collagen type I dishes, expression of BCR-FLTm1 did not result in enhanced expression of ATF3 in NP31 cells at protein levels. Nor could we find ATF3 induction in human umbilical vein endothelial cells that were stimulated by VEGF (data not shown). However, the fact that tubulogenesis is always accompanied by induced expression of ATF3 urged us to directly test its biological significance by siRNA-mediated gene knockdown.

The ATF3 induction by Matrigel was successfully inhibited by anti-ATF3 siRNA as shown in Fig. 1A (lane 4 versus 6) in tubulogenic NP31/kinase cells. To ensure the specificity of siRNAs, we have utilized two different controls: one is sense/sense primers for ATF3 (lane 5) and the other is antisense/sense primers for Nox1 (irrelevant siRNA) (lane 7). To our surprise, anti-ATF3 siRNA-treated cells no longer formed tubules in Matrigel, while cells with control RNAs did so (Fig.

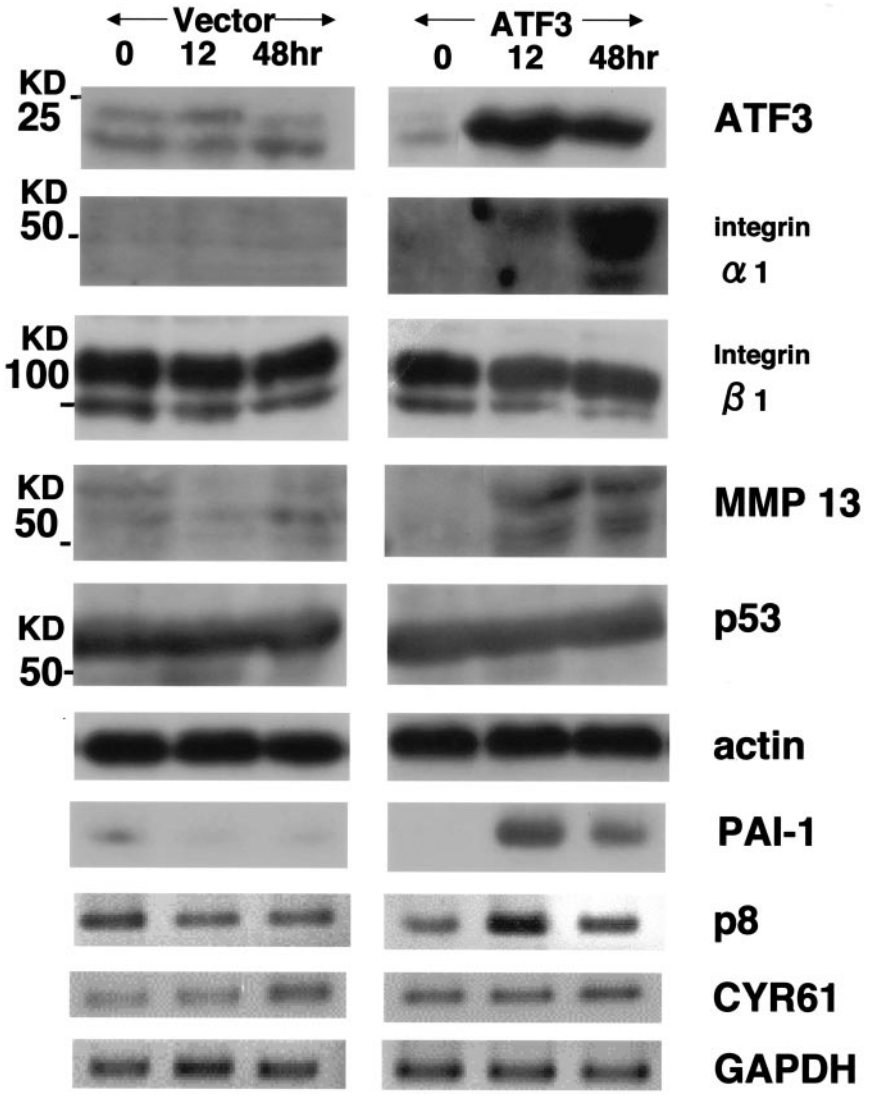

FIG. 4. Western (ATF3, integrin α1 subunit, integrin β1 subunit, MMP13, p53, and actin) and RT-PCR (PAI-1, p8, CYR61, and GAPDH) analyses of a set of cells shown in Fig. 3C. Representative results from three independent experiments are shown.

1B, C). Anti-Nox1 siRNAs did reduce the expression of Nox1 but not ATF3 (Fig. 1A, lane 7) without affecting tubulogenesis, as we described previously (19). This indicates that ATF3 induction is required for Matrigel-stimulated tubulogenesis in NP31/kinase cells that are programmed to form tubules.

Regulated expression of ATF3 in NP31 cells. We then tried to address the issue of whether or not ATF3 alone is capable of inducing angiogenesis. The full-length rat ATF3 cDNA was isolated from Matrigel-stimulated NP31/kinase cells, and was expressed under the control of a tetracycline (Tet)-regulated element (NP31/ATF3-Tet cells). Tet-regulated expression of the ATF3 protein on usual collagen plates was successful and achieved a maximum level of expression 12 h after induction, which was approximately 10-fold over that of the baseline as judged by densitometric analysis (Fig. 2A). Those cells showed no apparent morphological changes after ATF3 induction on usual culture dishes. However, when they were plated onto Matrigel 12 h after induction, they exhibited network formation with a lumen as shown in Fig. 2B and C. The tubulogenic ability of NP31/ATF3-Tet cells was evident when ATF3 was induced for at least 6 h before plating onto Matrigel, suggesting that a certain threshold in terms of both time and expression level may exist for NP31 cells to be ready for tubule formation in Matrigel.

Growth suppression by the induced expression of ATF3. The effect of ATF3 on cell growth has been under debate and appears to depend on cell types. This prompted us to test it in the background of endothelial cells. We found that cell growth was suppressed when ATF3 was induced in NP31/ATF3-Tet cells (Fig. 3A). The suppressive effect was also prominent when Tet-regulated ATF3 expression was achieved in the transformed NP31/kinase cells (NP31/kinase/ATF3-Tet cells) (Fig. 3B). Expression levels of cyclin-dependent protein kinase 4 (CDK4) and CDK2 were found to be decreased (Fig. 3C). However, those of CDK inhibitors remained unchanged, which include p27, p21 (data not shown), and p16 (Fig. 3C).

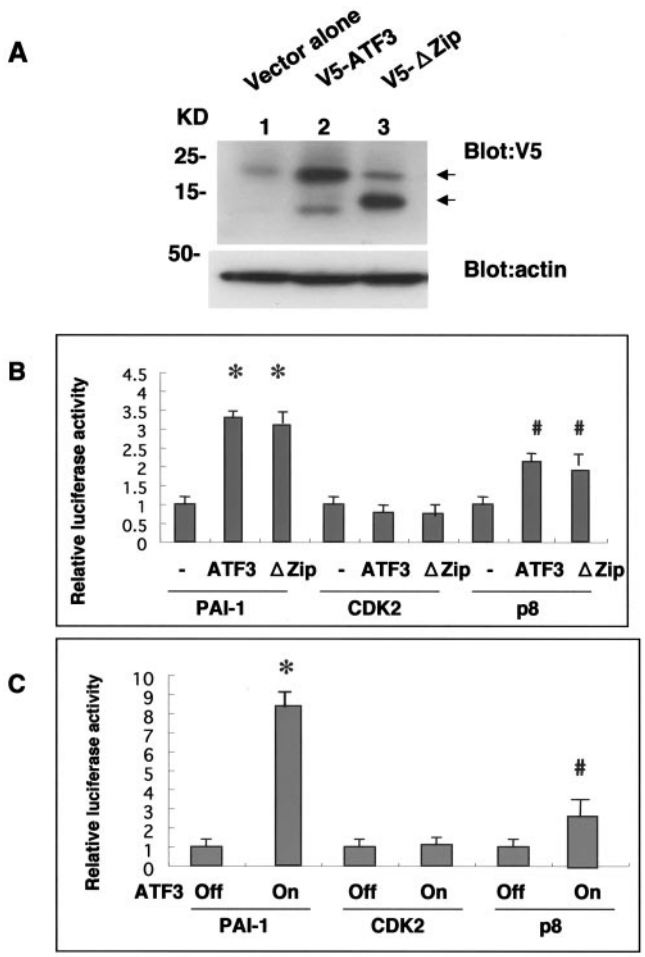

FIG. 5. (A) Total cell lysates from COS7 cells transiently transfected with vector alone (lane 1), V5-tagged full-length ATF3 (V5-ATF3, lane 2), or ATF3 mutant devoid of the leucine zipper domain (V5-ΔZip, lane 3) were subjected to anti-V5 (upper panel, arrows indicate V5-ATF3 and V5-ΔZip proteins) and antiactin (lower panel) Western blotting. (B) Relative luciferase activity in COS7 cells transfected with the same set of ATF3 constructs (−, vector alone) shown in panel A in combination with reporter plasmids for PAI-1, CDK2, or p8. Means ± SD of results from eight independent experiments are shown. *, $P < 0.05$ versus PAI-1 reporter alone; #, $P < 0.05$ versus p8 reporter alone. (C) Relative luciferase activity in NP31/ATF3-Tet cells transfected with the same set of reporter plasmids shown in panel B before (ATF3-Off) and after (ATF3-On) ATF3 induction. Means ± SD of results from eight independent experiments are shown. *, $P < 0.05$ versus PAI-1 reporter alone; #, $P < 0.05$ versus p8 reporter alone.

Direct analysis of gene expression in NP31/ATF3-Tet cells. We tried to identify a set of genes whose expression is directly regulated by ATF3 in this in vitro angiogenesis system. We initially examined the genes whose expression was already shown to be either up- or down-regulated when ATF3 was up-regulated by Matrigel in NP31/kinase cells in our previous results of microarray analysis (18). The up-regulated genes included integrin subunit α1, colony-stimulating factor 3 (csf3), p8, matrix Gla protein, and metallothionein 1, and down-regulated genes included p38 mitogen-activated protein kinase, heat shock protein 70, hsp90, and CYR61 (24). We also analyzed genes which are thought to be involved in angiogenesis or diabetic complications, including VEGF, matrix metalloprotease 2 (MMP2), MMP9, MMP10, MMP13, KDR (VEGFR-2), CD31, p53, PAI-1, receptor for advanced glycation end products (28), and Id1 (14). The expression level of none of the down-regulated genes in the microarray was altered. Integrin α1 subunit, p8, PAI-1, and MMP13 were the only genes that were found to be up-regulated in an ATF3-dependent manner (Fig. 4). The peak of expression of integrin α1 subunit and MMP13 was at 48 h after ATF3 induction, and expression levels decreased thereafter.

ATF3 affects promoter activity of PAI-1 and p8. To examine the ATF3 activity on transcription more directly, we performed reporter assays in two different ways. First, COS7 cells were transfected with V5-tagged full-length ATF3 or its mutant (ΔZip) that lacks the leucine zipper domain assumed to be responsible for DNA binding. We could repeatedly detect both of the proteins at equivalent expression levels (Fig. 5A).

Cotransfection of the ATF3 constructs with reporter plasmids for PAI-1, CDK2, or p8 gave significant elevations of luciferase activity in PAI-1 and p8 (Fig. 5B). Deletion of the leucine zipper did not affect the activity. Second, we transfected the reporter plasmids in NP31/ATF3-Tet cells (Fig. 2) before and after induction of ATF3. Significant enhancement of luciferase activity after induction was observed in PAI-1 and p8. The CDK2 promoter activity was found to be unaltered with statistical significance in both COS7 and NP31/ATF3-Tet cell transfections.

H_2O_2-induced ATF3 expression and network formation in NP31 cells. Growth factors that stimulate ATF3 induction include TNF-α, epidermal growth factor, hepatocyte growth factor, hydrogen peroxide (H_2O_2), and TGF-β (11, 13, 14, 16). NP31 cells failed to respond to epidermal growth factor or hepatocyte growth factor, as reported before (21). TNF-α and H_2O_2, but not TGF-β, enhanced ATF3 expression (Fig. 6A), and this is in agreement with our microarray analysis results reported before (18). Maximum expression levels of ATF3 proteins were 3.5- and 3.0-fold over the baseline level before stimulation with TNF-α and H_2O_2, respectively, as judged by densitometric analysis. Neither apoptosis nor network formation in Matrigel was observed in TNF-α-treated NP31 cells. Oxidative stress, an especially low concentration of H_2O_2, has been reported to induce in vitro angiogenesis (40). However, plating onto Matrigel killed almost all cells in 8 to 10 h when they had been pretreated with H_2O_2 for more than 6 h. Pretreatment for 1.5 h gave network formation as usual, although a small number of cells appeared apoptotic (compare Fig. 6C and Fig. 1B). Anti-ATF3 siRNA transfection before H_2O_2 pretreatment reduced the ATF3 expression at protein levels by roughly 50% (Fig. 6B) and inhibited the network formation by 62.3% (Fig. 6C and D), underscoring the ATF3 function as an important determinant in oxidative stress-induced angiogenesis.

Increased expression of ATF3 in OLETF diabetic model rats. We have previously reported ROS-dependent expression of PAI-1 in adipocytes of OLETF diabetic rats (42). The induced expression of PAI-1 by ATF3 in NP31/ATF3-Tet cells prompted us to analyze the ATF3 expression in H_2O_2-stimulated NP31 cells as shown in Fig. 6A. The protein level of ATF3 expression peaked within 1 h after stimulation. How-

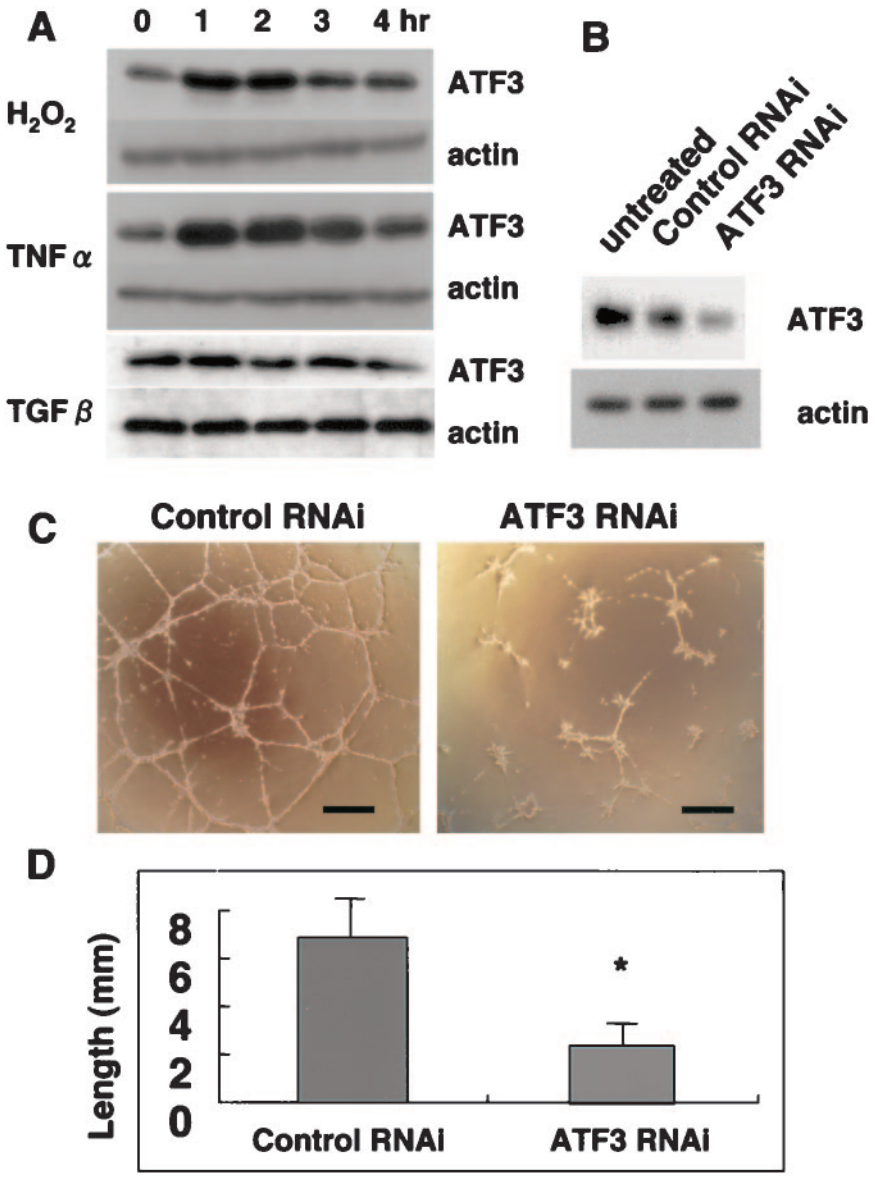

FIG. 6. (A) NP31 cells were treated with hydrogen peroxide (H_2O_2), TNF-α, or TGF-β for the indicated time in hours before total protein lysates were subjected to anti-ATF3 (upper panel) and antiactin (lower panel) Western blotting. (B) NP31 cells were left untreated or pretreated with anti-ATF3 siRNA (antisense/sense) or control RNA interference (RNAi; sense/sense) and then stimulated with H_2O_2 for 1.5 h. ATF3 expression was analyzed as in panel A. (C) NP31 cells transfected with anti-ATF3 siRNA or control RNAi shown in panel B were subjected to Matrigel assays. Bars, 100 μm. (D) Quantification of in vitro tubulogenesis shown in panel C. Means ± SD of results from four independent experiments are shown. *, $P < 0.05$ versus control RNAi.

ever, the peak of mRNA expression of both PAI-1 and p8 took place 4 h after stimulation (Fig. 7A).

Then we analyzed their expression in all the organs and tissues in the animals. First, comparative RT-PCR analysis of ATF3 mRNA expression between OLETF and control LETO rats was performed in organs including the brain, retina, heart, aorta, lung, whole kidney, glomerulus, liver, sinusoidal endothelial cells, spleen, and pancreas. Although only subtle changes have been histopathologically observed in those animals (26, 36), we could repeatedly detect increased mRNA expression of ATF3 in the glomerulus of OLETF rats (Fig. 7B). We could also detect concomitant elevation of PAI-1 and p8 expression in the glomerulus. Although ATF3 expression was only slightly, but appreciably, increased in the aorta of OLETF relative to LETO rats, expression levels of both PAI-1 and p8 were found to be significantly augmented (Fig. 7B). We could also observe that expression levels of PAI-1 proteins in the glomerulus were higher in OLETF than LETO rats (Fig. 7C).

To examine the cell type that is involved in the elevated ATF3 expression in OLETF rats, histological sections from each organ or tissue were subjected to immunostaining with anti-ATF3 antibody. Increased expression of ATF3 observed in the glomerulus was colocalized with CD31-positive staining,

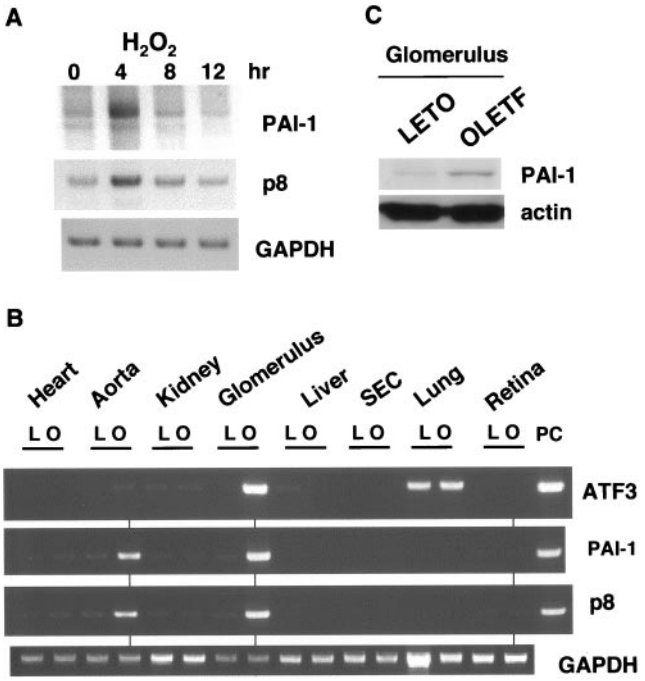

FIG. 7. (A) RT-PCR analysis of PAI-1 and p8 in NP31 cells treated with H_2O_2 shown in Fig. 6. (B) RT-PCR analysis of mRNAs from heart, aorta, whole kidney, glomerulus prepared from kidney, whole liver, and sinusoidal endothelial cells (SEC) from liver, lung, and retina in OLETF (O) and control LETO (L) rats. PC, control plasmid DNAs for each gene. Representative results from four independent experiments are shown. (C) Total protein lysates from glomeruli of LETO or OLETF rats were subjected to anti-PAI-1 and antiactin Western blotting.

suggesting that ATF3 expression is increased in glomerular endothelial cells (Fig. 8A and B). PAI-1 expression in the glomerulus was observed in both LETO and OLETF rats and merged with CD31 expression (Fig. 8C). Increased expression of ATF3 was also detected in endothelial cells of aorta from OLETF rats (Fig. 8D).

DISCUSSION

In physiological circumstances, the mRNA level of ATF3 is relatively low in most cell types. Induction of ATF3 mRNA by stress signals such as mechanical injury, chemicals, ischemia/reperfusion, and so forth, is an early event and it returns to a low level after several hours (6). However, in pathological settings, persistent expression of ATF3 at a moderate to high degree has been documented. ATF3 is highly expressed in vascular endothelial cells in the atherosclerotic lesion and implicated in cell death (27).

While ATF3 was reported to suppress cell growth in HeLa cells by blocking G_1-S progression (9), there have been at least four studies that showed growth-promoting activity of ATF3 (2, 29, 33, 41). ATF3 was found to be downstream of c-Myc and adenovirus-mediated overexpression of ATF3 in c-Myc-deficient fibroblasts resulted in increased CDK4 and CDK2 activity (41). Our in vitro analysis of NP31/ATF3-Tet cells has revealed that ATF3 alone could induce growth suppression and tubulogenic differentiation in endothelial cells. Since c-Myc induction was not observed in our in vitro tubulogenesis system (data not shown), it can safely be said that ATF3-mediated control of cell growth depends on cell type and context. The sequence of our anti-ATF3 siRNA that inhibited tubulogenesis by NP31/kinase cells is within the repression region, and therefore, all isoforms of ATF3 (5, 12, 31, 46) could be targeted. Establishment of NP31/ATF3-Tet cells individually expressing the different isoforms might answer the question of which isoform(s) can induce tubulogenesis.

Forced expression of ATF3 in NP31/ATF3-Tet cells was accompanied by up- or down-regulation of potentially angiogenic genes/proteins, including integrin α1 subunit, MMP13, PAI-1, and p8 (Fig. 9). Anti-α1 blocking antibody was shown to inhibit angiogenesis (38). Diabetic nephropathy was shown to be associated with mesangial hypertrophy with strong induction of p8 (10). Although the precise function of p8 is still unknown, a higher level of CDK2 and CDK4 was observed in p8-deficient cells and p8 mRNA was elevated after growth arrest induced by serum deprivation (44). This would concur with our findings in the endothelial background that ATF3 regulated both CDK and p8 expression levels. TNF-α was shown to stimulate PAI-1 gene expression in a variety of organs, including the liver (37). Given that our experiments showed that PAI-1 is induced by ATF3 and ATF3 is induced by TNF-α in NP31 cells, it could also be possible that PAI-1 is induced by stress stimuli in an ATF3-dependent fashion. MMP13 has recently been shown to play a significant role for tumor cells to invade in Matrigel (1). ATF3 has been shown to repress MMP2 expression in human fibrosarcoma HT1080 cells (47). However, we have previously reported the increased expression as well as activation of MMP2 in NP31/kinase cells in Matrigel cultures (23). Given the repeated failure in induction of MMP2 gene expression in NP31/ATF3-Tet cells in usual liquid cultures, it is possible that the molecule(s) responsible for its induction could be other transcription factor that is activated by Matrigel in NP31/kinase cells.

Precise mechanisms of ATF3-mediated regulation of expression of those genes stated above still remain to be investigated further. NP31 cells expressing the V5-tagged ATF3 mutant devoid of the leucine zipper domain (ATF3ΔZip) failed to form tubules in Matrigel (data not shown). However, ATF3ΔZip still retained the ability to stimulate transcription from the PAI-1 and p8 promoters. One hypothesis could be that it is due to corepressor-binding activity to sequester the unknown corepressors from the promoter (5, 31). Alternatively, some unknown genes essential for tubulogenesis might be activated in a leucine zipper-dependent manner. In our experiments, the leucine zipper-dependent expression was observed only in MMP2 by transient transfection of COS7 cells (data not shown). Again we need to underline that ATF3-mediated gene expression depends on cellular context. cDNA microarray analysis of NP31/ATF3-Tet and NP31/ATF3ΔZip-Tet cells before and after Tet deprivation may be an interesting future experiment.

In diabetic angiopathy, hyperglycemia-induced ROS production causes oxidative stress in endothelial cells (4). The H_2O_2 precursor, superoxide, is produced by Nox family members. We have recently shown that NP31 cells overexpressing Nox1 were capable of forming immature tubules without a lumen in Matrigel cultures (19). However, NP31/ATF3-Tet

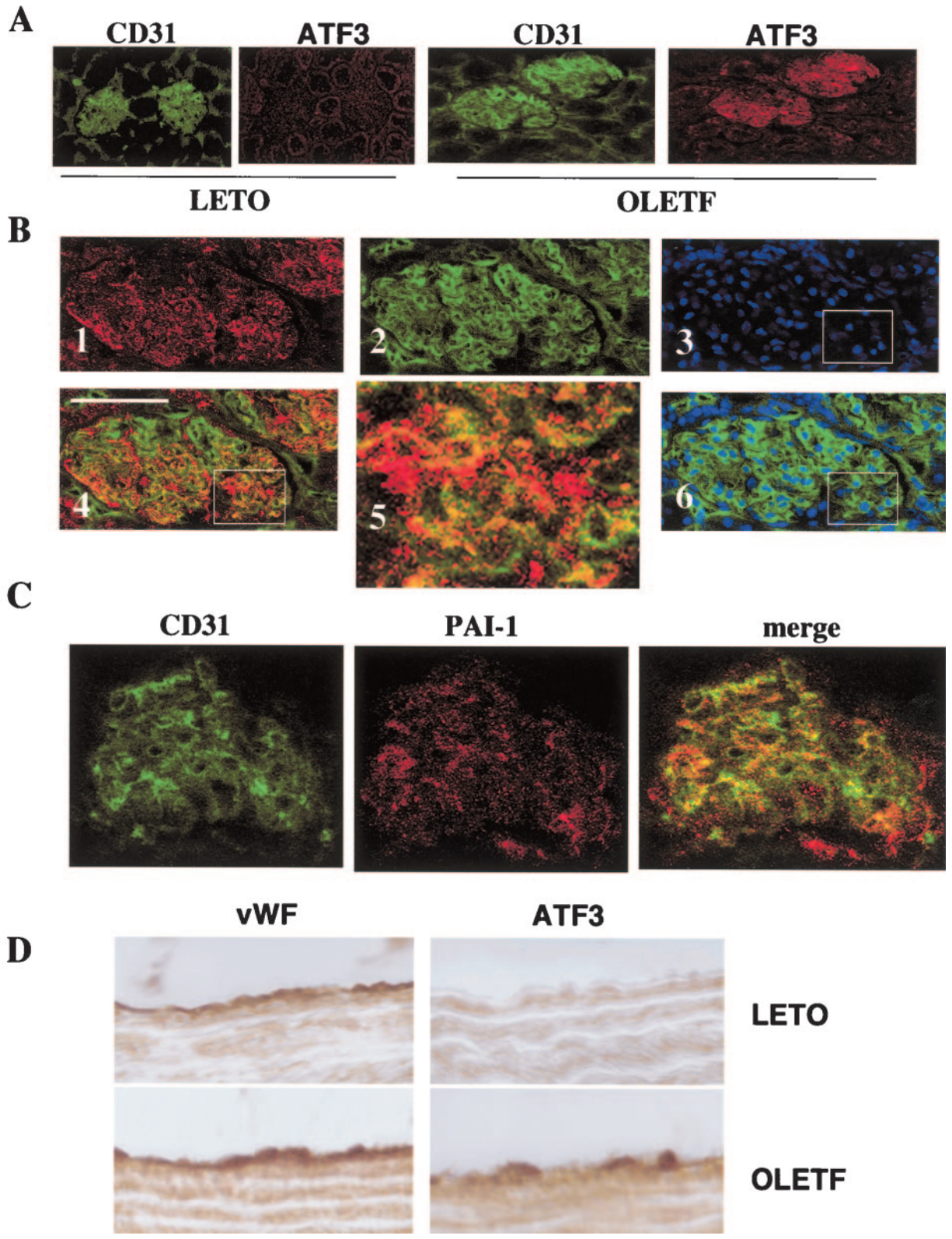

FIG. 8. (A) Anti-ATF3 and anti-CD31 immunostaining of glomeruli from LETO and OLETF rats. (B) Immunostaining of the OLETF glomerulus with anti-ATF3 (1), anti-CD31 (2), and PI (3) and merged images for ATF3 and CD31 (4) and PI and CD31 (6). The boxed area in panel 4 is shown in higher magnification in panel 5. (C) Anti-CD31 and anti-PAI-1 immunostaining and their merged image in the glomerulus from OLETF rats. (D) Endothelial cells of aorta from LETO and OLETF rats were stained with anti-von Willebrand factor (vWF) or anti-ATF3 antibody.

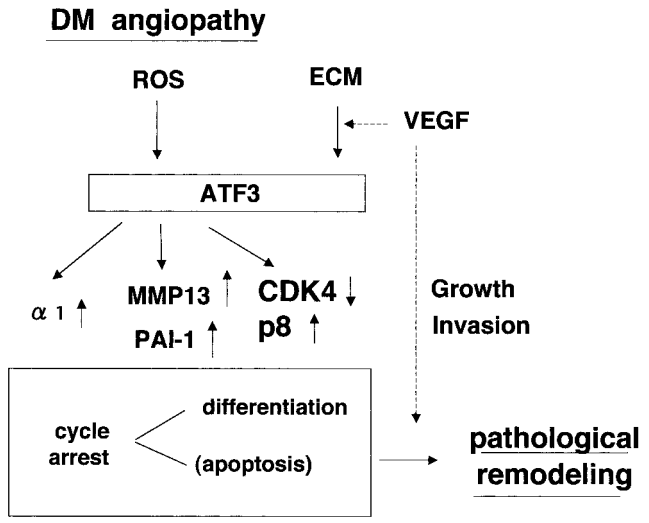

FIG. 9. A hypothetical scheme of ROS-induced pathological angiogenesis in microvascular disorders in diabetes mellitus (DM). ATF3 may be persistently and highly induced by ROS or a certain component(s) of the extracellular matrix (ECM), which results in cell cycle arrest and differentiation. In some conditions, cells cannot tolerate ROS attacks and undergo apoptosis. Those processes could take place in a VEGF-independent manner. However, we assume that actual angiogenic remodeling occurs by the repeated action of differentiation program and growth factors such as VEGF that promotes dedifferentiation.

cells formed a lumen in Matrigel when ATF3 was induced. Therefore we suppose that other factors activated by ROS, such as NF-κB, could have biological effects in addition to those of ATF3 (20) and vise versa.

The building of epithelial architecture is supposed to be guided by two elements: an intrinsic differentiation program that drives maturation of morphological differentiation such as lumen formation and a growth factor-induced dedifferentiation that transiently allows cell proliferation and subsequent remodeling of the architecture (30). ATF3 has been reported to enhance cell differentiation such as neurite sprouting (32). Our data provide evidence for participation of ATF3 in oxidative stress-induced tubulogenic differentiation of endothelial cells. The ATF3-mediated switch from an activated to repressive state in terms of cell growth may be caused by altered expression levels of cell cycle regulators. Endothelial cells that evade apoptosis induced by oxidative stress could restore growth by growth factors such as VEGF. This raises an idea that those opposing processes repeated in tandem could be pathologically modified by ATF3 in diabetic angiopathy, leading to abnormal vascular remodeling (Fig. 9). The hypothesis needs to be tested with human samples from diabetic patients.

ACKNOWLEDGMENTS

We thank O. N. Witte at the University of California—Los Angeles for the Tet constructs, Otsuka Pharmaceutical Co. for the OLETF animals, and S. Kobayashi for technical help. We also thank S. Fujii at Hokkaido University for providing PAI-1 promoter constructs and S. Morikawa for technical help in confocal microscopy.

This work is supported by a grant-in-aid for scientific research on metal sensors (no. 12147210) from the Japanese government.

REFERENCES

1. **Ala-aho, R., M. Ahonen, S. J. George, J. Heikkila, R. Grenman, M. Kallajoki, and V. M. Kahari.** 2004. Targeted inhibition of human collagenase-3 (MMP-13) expression inhibits squamous cell carcinoma growth in vivo. Oncogene **23:**5111–5123.
2. **Allan, A. L., C. Albanese, R. G. Pestell, and J. LaMarre.** 2001. Activating transcription factor 3 induces DNA synthesis and expression of cyclin D1 in hepatocytes. J. Biol. Chem. **276:**27272–27280.
3. **Benezra, R., S. Rafil, and D. Lyden.** 2001. The Id proteins and angiogenesis. Oncogene **20:**8334–8341.
4. **Brownlee, M.** 2001. Biochemistry and molecular cell biology of diabetic complications. Nature **414:**813–820.
5. **Chen, B. P. C., G. Liang, J. Whelan, and T. Hai.** 1994. ATF3 and ATF3ΔZip. Transcriptional repression versus activation by alternatively spliced isoforms. J. Biol. Chem. **269:**15819–15826.
6. **Chen, B. P. C., C. D. Wolfgang, and T. Hai.** 1996. Analysis of ATF3, a transcription factor induced by physiological stresses and modulated by gadd153/Chop10. Mol. Cell. Biol. **16:**1157–1168.
7. **Dong, J., S. Fujii, H. Li, H. Nakabayashi, M. Sakai, S. Nishi, D. Goto, T. Furumoto, S. Imagawa, T. A. K. M. Zaman, and A. Kitabatake.** 2005. Interleukin-6 and mevastatin regulate plasminogen activator inhibitor-1 through CCAAT/enhancer-binding protein-δ. Arterioscler. Thromb. Vasc. Biol. **25:**1078–1084.
8. **Era, T., and O. N. Witte.** 2000. Regulated expression of P210 Bcr-Abl during embryonic stem cell differentiation stimulates multipotential progenitor expansion and myeloid cell fate. Proc. Natl. Acad. Sci. USA **97:**1737–1742.
9. **Fan, F., S. Jin, S. A. Amundson, T. Tong, W. Fan, H. Zhao, X. Zhu, L. Mazzacurati, X. Li, K. L. Petrik, A. J. Fornace, Jr., B. Rajasekaran, and Q. Zhan.** 2002. ATF3 induction following DNA damage is regulated by distinct signaling pathways and over-expression of ATF3 protein suppresses cells growth. Oncogene **21:**7488–7496.
10. **Goruppi, S., J. V. Bonventre, and J. M. Kyriakis.** 2002. Signaling pathways and late-onset gene induction associated with renal mesangial cell hypertrophy. EMBO J. **21:**5427–5436.
11. **Hai, T., C. D. Wolfgang, D. K. Marsee, A. E. Allen, and U. Sivaprasad.** 1999. ATF3 and stress responses. Gene Expr. **7:**321–335.
12. **Hashimoto, Y., C. Zhang, J. Kawauchi, I. Imoto, M. T. Adachi, J. Inazawa, T. Amagasa, T. Hai, and S. Kitajima.** 2002. An alternatively spliced isoform of transcriptional repressor ATF3 and its induction by stress stimuli. Nucleic Acids Res. **30:**2398–2406.
13. **Inoue, K., T. Zama, T. Kamimoto, R. Aoki, Y. Ikeda, H. Kimura, and M. Hagiwara.** 2004. TNF-α induced ATF3 expression is bidirectionally regulated by the JNK and ERK pathways in vascular endothelial cells. Genes Cells **9:**59–70.
14. **Kang, Y., C. R. Chen, and J. Massagué.** 2003. A self-enabling TGFβ response coupled to stress signaling: Smad engages factor ATF3 for Id1 repression in epithelial cells. Mol. Cell **11:**915–926.
15. **Karnovsky, M. J., and G. B. Ryan.** 1975. Structure of the glomerular slit diaphragm in freeze-fractured normal rat kidney. J. Cell Biol. **65:**233–236.
16. **Kawauchi, J., C. Zhang, K. Nobori, Y. Hashimoto, M. T. Adachi, A. Noda, M. Sunamori, and S. Kitajima.** 2002. Transcriptional repressor activating transcription factor 3 protects human umbilical vein endothelial cells from tumor necrosis factor-α-induced apoptosis through down-regulation of p53 transcription. J. Biol. Chem. **277:**39025–39034.
17. **Khatri, J. J., C. Johnson, R. Magid, S. M. Lessner, K. M. Laude, S. I. Dikalov, D. G. Harrison, H. J. Sung, Y. Rong, and Z. S. Galis.** 2004. Vascular oxidant stress enhances progression and angiogenesis of experimental atheroma. Circulation **109:**520–525.
18. **Kobayashi, S., E. Ito, R. Honma, Y. Nojima, M. Shibuya, S. Watanabe, and Y. Maru.** 2004. Dynamic regulation of gene expression by the Flt-1 kinase and Matrigel in endothelial tubulogenesis. Genomics **84:**185–192.
19. **Kobayashi, S., Y. Nojima, M. Shibuya, and Y. Maru.** 2004. Nox1 regulates apoptosis and potentially stimulates branching morphogenesis in sinusoidal endothelial cells. Exp. Cell Res. **300:**455–462.
20. **Li, N., and M. Karin.** 1999. Is NF-κB the sensor of oxidative stress? FASEB J. **13:**1137–1143.
21. **Maru, Y., S. Yamaguchi, T. Takahashi, H. Ueno, and M. Shibuya.** 1998. Virally activated Ras cooperates with integrin to induce tubulogenesis in sinusoidal endothelial cell lines. J. Cell. Physiol. **176:**223–234.
22. **Maru, Y., S. Yamaguchi, and M. Shibuya.** 1998. Flt-1, a receptor for vascular endothelial growth factor, has transforming and morphogenic potentials. Oncogene **16:**2585–2595.
23. **Maru, Y., H. Hirosawa, and M. Shibuya.** 2000. An oncogenic form of the Flt-1 kinase has a tubulogenic potential in a sinusoidal endothelial cell line. Eur. J. Cell Biol. **79:**130–143.
24. **Mo, F. E., A. G. Muntean, C. C. Chen, D. B. Stolz, S. C. Watkins, and L. F. Lau.** 2002. CYR61 (CCN1) is essential for placental development and vascular integrity. Mol. Cell. Biol. **22:**8709–8720.
25. **Moeller, B. J., Y. Cao, C. Y. Li, and M. W. Dewhirst.** 2004. Radiation activates HIF-1 to regulate vascular radiosensitivity in tumors: role of reoxygenation, free radicals, and stress granules. Cancer Cell **5:**429–441.

26. **Mori, S., K. Kawano, T. Hirashima, and T. Natori.** 1996. Relationships between diet control and the development of spontaneous type II diabetes and diabetic nephropathy in OLETF rats. Diabetes Res. Clin. Pract. **33:**145–152.
27. **Nawa, T., M. T. Nawa, M. T. Adachi, I. Uchimura, R. Shimokawa, K. Fujisawa, A. Tanaka, F. Numano, and S. Kitajima.** 2002. Expression of transcriptional repressor ATF3/LRF1 in human atherosclerosis colocalization and possible involvement in cell death of vascular endothelial cells. Atherosclerosis **16:**281–291.
28. **Neeper, M., A. M. Schmidt, J. Brett, S. D. Yan, F. Wang, Y. C. Pan, K. Elliston, D. Stern, and A. Shaw.** 1992. Cloning and expression of a cell surface receptor for advanced glycosylation end products of proteins. J. Biol. Chem. **267:**14998–15004.
29. **Nilssen, L. S., J. Ødegård, G. H. Thoresen, A. Molven, D. Sandnes, and T. Christoffersen.** 2004. G protein-coupled receptor agonist-stimulated expression of ATF3/LRF-1 and c-myc and comitogenic effects in hepatocytes do not require EGF receptor transactivation. J. Cell. Physiol. **201:**349–358.
30. **O'Brien, L. E., M. M. Zegers, and K. E. Mostov.** 2002. Building epithelial architecture: insights from three-dimensional culture models. Nat. Rev. Mol. Cell Biol. **3:**531–537.
31. **Pan, Y., H. Chen, F. Siu, and M. S. Kilberg.** 2003. Amino acid deprivation and endoplasmic reticulum stress induce expression of multiple activating transcription factor-3 mRNA species that, when overexpressed in HepG2 cells, modulate transcription by the human asparagine synthetase promoter. J. Biol. Chem. **278:**38402–38412.
32. **Pearson, A. G., C. W. Gray, J. F. Pearson, J. M. Greenwood, M. J. During, and M. Dragunow.** 2003. ATF3 enhances c-Jun mediated neurite sprouting. Mol. Brain Res. **120:**38–45.
33. **Perez, S., E. Vial, V. H. Dam, and M. Castellazzi.** 2001. Transcription factor ATF3 partially transforms chick embryo fibroblasts by promoting growth factor-independent proliferation. Oncogene **20:**1135–1141.
34. **Ploplis, V. A., R. Balsara, M. J. Sandoval-Cooper, Z. J. Yin, J. Betten, N. Modi, D. Gadoua, D. Donahue, J. A. Martin, and F. J. Castellino.** 2003. Enhanced *in vitro* proliferation of aortic endothelial cells from plasminogen activator inhibitor-1-deficient mice. J. Biol. Chem. **279:**6143–6151.
35. **Qian, Y., J. Luo, S. S. Leonard, G. K. Harris, L. Millecchia, D. C. Flynn, and X. Shi.** 2003. Hydrogen peroxide formation and actin filament reorganization by Cdc42 are essential for ethanol-induced *in vitro* angiogenesis. J. Biol. Chem. **278:**16189–16197.
36. **Saito, F., M. Kawaguchi, J. Izumida, T. Asakura, K. Maehara, and Y. Maruyama.** 2003. Alteration in haemodynamics and pathological changes in the cardiovascular system during the development of type 2 diabetes mellitus in OLETF rats. Diabetologia **46:**1161–1169.
37. **Sawdey, M. S., and D. J. Loskutoff.** 1991. Regulation of murine type 1 plasminogen activator inhibitor gene expression in vivo. Tissue specificity and induction by lipopolysaccharide, tumor necrosis factor-alpha, and transforming growth factor-beta. J. Clin. Investig. **88:**1346–1353.
38. **Senger, A. P., K. P. Claffey, J. E. Benes, C. A. Perruzzi, A. P. Sergiou, and M. Detmar.** 1997. Angiogenesis promoted by vascular endothelial growth factor: regulation through $\alpha1\beta1$ and $\alpha2\beta1$ integrins. Proc. Natl. Acad. Sci. USA **94:**13612–13617.
39. **Stennett, L. S., A. I. Riker, T. M. Kroll, J. Chamberlin, T. Miki, B. J. Nickoloff, and I. C. Le Poole.** 2004. Expression of gp100 and CDK2 in melanoma cells is not coregulated by a shared promoter region. Pigment Cell Res. **17:**525–532.
40. **Stone, J. R., and J. Collins.** 2002. The role of hydrogen peroxide in endothelial proliferative responses. Endothelium **9:**231–238.
41. **Tamura, K., B. Hua, S. Adachi, I. Guney, J. Kawauchi, M. Morioka, M. Tamamori-Adachi, Y. Tanaka, Y. Nakabeppu, M. Sunamori, J. M. Sedivy, and S. Kitajima.** 2005. Stress response gene ATF3 is a target of c-myc in serum-induced cell proliferation. EMBO J. **24:**2590–2601.
42. **Uchida, Y., K. Ohba, T. Yoshioka, K. Irie, T. Muraki, and Y. Maru.** 2004. Cellular carbonyl stress enhances the expression of plasminogen activator inhibitor-1 in rat white adipocytes via reactive oxygen species-dependent pathway. J. Biol. Chem. **279:**4075–4083.
43. **Vasseur, S., G. V. Mallo, A. Garcia-Montero, E. M. Ortiz, F. Fiedler, E. Canepa, S. Moreno, and J. L. Iovanna.** 1999. Structural and functional characterization of the mouse p8 gene: promotion of transcription by the CAAT-enhancer binding protein α (C/EBPα) and C/EBPβ trans-acting factors involves a C/EBP cis-acting element and other regions of the promoter. Biochem. J. **343:**377–383.
44. **Vasseur, S., A. Hoffmeister, A. Garcia-Montero, G. V. Mallo, R. Feil, S. Kühbandner, J. C. Dagorn, and J. L. Iovanna.** 2002. p8-deficient fibroblasts grow more rapidly and are more resistant to adriamycin-induced apoptosis. Oncogene **21:**1685–1694.
45. **Volpert, O. V., R. Pili, H. A. Sikder, T. Nelius, T. Zaichuk, C. Morris, C. B. Shiflett, M. K. Devlin, K. Conant, and R. M. Alani.** 2002. Id1 regulates angiogenesis through transcriptional repression of thrombospondin-1. Cancer Cell **2:**473–483.
46. **Wang, J., Y. Cao, and D. F. Steiner.** 2003. Regulation of proglucagon transcription by activated transcription factor (ATF)3 and a novel isoform, ATF3b, through the cAMP-response element/ATF site of the proglucagon gene promoter. J. Biol. Chem. **278:**32899–32904.
47. **Yan, C., H. Wang, and D. D. Boyd.** 2002. ATF3 represses 72-kDa type IV collagenase (MMP-2) expression by antagonizing p53-dependent trans-activation of the collagenase promoter. J. Biol. Chem. **277:**10804–10812.